

摩擦学学报

TRIBOLOGY



不同NiCr含量的NiCr-Cr₃C₂涂层高温冲击磨损行为研究

耿少寅, 王浩宇, 何斌, 曹晓英, 王伟, 巩秀芳, 蔡振兵

Impact Wear Behavior of NiCr-Cr₃C₂ Coatings with Different NiCr Contents at High Temperature

GENG Shaoyin, WANG Haoyu, HE Bin, CAO Xiaoying, WANG Wei, GONG Xiufang, CAI Zhenbing

在线阅读 View online: <https://doi.org/10.16078/j.tribology.2023155>

您可能感兴趣的其他文章

Articles you may be interested in

高承载高耐磨Cr₃C₂-NiCr/DLC复合涂层制备及摩擦学行为

Preparation and Tribological Behavior of Cr₃C₂-NiCr/DLC Duplex Coating with High Load-Bearing and Wear Resistance

摩擦学学报. 2022, 42(4): 751 <https://doi.org/10.16078/j.tribology.2021274>

2种Zr(-Sn)-Nb合金与316L不锈钢的冲击磨损性能

Impact Wear Properties of Two Zr(-Sn)-Nb Zirconium Alloys with 316L Stainless Steel

摩擦学学报. 2023, 43(8): 868 <https://doi.org/10.16078/j.tribology.2022125>

冲击载荷下Al₂O₃磨料对齿轮磨损行为的作用机理研究

Action Mechanism of Al₂O₃ Abrasive on Gear Wear Behavior under Impact Load

摩擦学学报. 2023, 43(6): 682 <https://doi.org/10.16078/j.tribology.2022046>

镍基Al_xCoCrFeNi高熵合金涂层升温摩擦性能的原子尺度分析

Molecular Dynamics Simulation of Al_xCoCrFeNi High Entropy Alloy Coating at High Temperature

摩擦学学报. 2024, 44(4): 530 <https://doi.org/10.16078/j.tribology.2023068>

C₂H₂/Ar流量比对a-C:H涂层结构及摩擦学性能的影响

Effect of C₂H₂/Ar Flow Rate on Microstructure and Tribological Properties of a-C:H Coatings

摩擦学学报. 2022, 42(3): 588 <https://doi.org/10.16078/j.tribology.2021029>



关注微信公众号, 获得更多资讯信息

耿少寅, 王浩宇, 何斌, 曹晓英, 王伟, 巩秀芳, 蔡振兵. 不同NiCr含量的NiCr-Cr₃C₂涂层高温冲击磨损行为研究[J]. 摩擦学学报(中英文), 2024, 44(9): 1192–1203. GENG Shaoyin, WANG Haoyu, HE Bin, CAO Xiaoying, WANG Wei, GONG Xiufang, CAI Zhenbing. Impact Wear Behavior of NiCr-Cr₃C₂ Coatings with Different NiCr Contents at High Temperature[J]. Tribology, 2024, 44(9): 1192–1203. DOI: 10.16078/j.tribology.2023155

不同NiCr含量的NiCr-Cr₃C₂涂层高温冲击磨损行为研究

耿少寅^{1,2}, 王浩宇², 何斌², 曹晓英¹, 王伟¹, 巩秀芳¹, 蔡振兵^{1,2*}

(1. 东方汽轮机有限公司 清洁高效透平动力装备全国重点实验室, 四川 德阳 618000;

2. 西南交通大学 摩擦学研究所, 四川 成都 610031)

摘要: 通过超音速火焰喷涂制备了35% NiCr-Cr₃C₂涂层及25% NiCr-Cr₃C₂涂层, 利用自研的高温铁屑冲击磨损试验机, 在630 °C及铁屑冲蚀的环境下进行了不同次数下的冲击试验(1×10⁴、2×10⁴和5×10⁴), 研究了2种涂层在铁屑冲蚀环境下的高温冲击磨损行为. 结果表明: 在高温铁屑环境下35% NiCr-Cr₃C₂涂层和25% NiCr-Cr₃C₂涂层的损伤机理均为塑性变形和磨粒磨损, 在相同冲击次数下两者的磨损面积相差不大, 但25% NiCr-Cr₃C₂涂层能量吸收量及吸收率和磨损体积均小于35% NiCr-Cr₃C₂涂层, 表现出了更好的耐高温冲击磨粒磨损性能; 随着冲击次数的增加, 2种涂层的冲击能量、能量吸收率及磨损面积均呈增长趋势, 表明2种涂层发生了更多的塑性变形和材料去除; 2种涂层的磨损体积随着冲击次数的增加呈现出不同的变化规律, 25% NiCr-Cr₃C₂涂层的磨损体积随冲击次数的增加而增加, 而35% NiCr-Cr₃C₂涂层的磨损体积则随冲击次数的增加呈现先增大再减小的规律.

关键词: NiCr-Cr₃C₂涂层; 高温铁屑冲击; 动力学响应; 冲击磨损

中图分类号: TH117.1; TG156

文献标志码: A

文章编号: 1004-0595(2024)09-1192-12

Impact Wear Behavior of NiCr-Cr₃C₂ Coatings with Different NiCr Contents at High Temperature

GENG Shaoyin^{1,2}, WANG Haoyu², HE Bin², CAO Xiaoying¹,
WANG Wei¹, GONG Xiufang¹, CAI Zhenbing^{1,2*}

(1. State Key Laboratory of Clean and Efficient Turbomachinery Power Equipment,
Dongfang Turbine Co., Sichuan Deyang 618000, China;

2. Tribology Research Institute, Southwest Jiaotong University, Sichuan Chengdu 610031, China)

Abstract: Steam turbine is a kind of power machinery that converts the heat energy generated by fuel combustion into mechanical energy for driving power generation, and is the key equipment of coal power units, nuclear power units, gas and steam cycle generating units and other units. In the actual work of the steam turbine, due to the influence of high temperature, high pressure steam, high pressure fluid, etc., the key components of the steam turbine are susceptible to corrosion, mechanical damage, impact wear and other problems. In order to extend the service life of these components, a protective coating is usually applied on the surface of the components by various processes. NiCr-Cr₃C₂ coating

Received 21 August 2023, revised 10 October 2023, accepted 11 October 2023, available online 19 April 2024.

*Corresponding author. E-mail: caizb@swjtu.cn, Tel: +86-15828457775.

This project was supported by Sichuan Science and Technology Planning Project (2022JDJQ0019, 2022ZYD0029) and Open Project of National Key Laboratory for Clean and Efficient Turbine Power Equipment.

四川省科技计划项目(2022JDJQ0019, 2022ZYD0029)和清洁高效透平动力装备全国重点实验室开放课题资助。

prepared by thermal spraying technology has excellent high temperature wear resistance and corrosion resistance, and has the potential to serve as a protective coating for turbine components. At present, there have been many studies on the properties of NiCr-Cr₃C₂ coating, but there are few reports on the impact wear behavior of this coating under high temperature environment. In this paper, 35% NiCr-Cr₃C₂ coating and 25% NiCr-Cr₃C₂ coating with different NiCr content were prepared by supersonic flame spraying. The real service condition of steam turbine was simulated by using a self-developed high-temperature iron chip impact wear tester. Impact tests (1×10^4 , 2×10^4 and 5×10^4) were carried out at 630 °C and under the environment of iron filings erosion. The impact wear behavior of the two coatings under the environment of iron filings erosion at high temperature was studied through the dynamic response during impact and the wear pattern after impact. The dynamic response data in the impact process mainly included the impact velocity curve and the impact force curve, which were collected by the corresponding sensor. The macroscopic morphology of the wear marks was observed by ultra depth of field optical microscope, and the microscopic morphology of the surface and cross section of the wear marks was observed by scanning electron microscope. The maximum wear depth and wear area and volume of the wear mark were obtained by measuring the contour of the wear mark with white light interferometer. The distribution of elements on the surface and cross section of the abrasion were analyzed by energy dispersive spectrometer. The results showed that the damage mechanisms of 35% NiCr-Cr₃C₂ coating and 25% NiCr-Cr₃C₂ coating were plastic deformation and abrasive wear, and the wear areas of the two coatings were not different under the same impact times. With the increase of impact times, the impact energy, energy absorption rate and wear area of the two coatings all showed an increasing trend, while the peak value of impact force showed a decreasing trend, that was, with the increase of impact times, more material removal and plastic deformation occurred in the two coatings. The wear volume of 25% NiCr-Cr₃C₂ coating increased with the increase of impact times, and under the same impact times, the energy absorption amount, absorption rate and wear volume of 25% NiCr-Cr₃C₂ coating were smaller than that of 35% NiCr-Cr₃C₂ coating, showing better resistance to high temperature impact wear. In the high temperature environment, the iron filings had good durability and were easy to be compacting by the impact ball and became the third body between the impact ball and the impact sample. As the formation of this third body would fill part of the pits on the wear marks, the wear volume of 35% NiCr-Cr₃C₂ coating would first increase and then decrease with the increase of impact times.

Key words: NiCr-Cr₃C₂ coating; high temperature impact with iron filings; dynamic response; impact wear

汽轮机是1种将燃料燃烧产生的热能转化为机械能用于驱动发电的动力机械,是煤电机组、核电机组、燃气与蒸汽循环发电机组等机组的关键设备^[1-3].在汽轮机的实际工作中由于高温、高压蒸汽和高压流体等的影响,导致汽轮机关键部件易受到腐蚀、机械损伤以及冲击磨损等问题的侵扰^[4-5],为了延长这些部件的使用寿命,通常采用各种工艺在部件表面涂上1层保护涂层,热喷涂技术因其喷制的涂层具有良好的耐磨性、耐腐蚀性及抗高温氧化性^[6],成为制备汽轮机保护涂层的常用技术之一.

碳化铬基硬质合金被认为是适用于热喷涂技术制备耐磨高温涂层的材料^[7],利用热喷涂技术制备的NiCr-Cr₃C₂涂层具有优良的高温耐磨和抗腐蚀性能,该涂层被广泛应用于工业领域中各种高温易磨部件上,其最高使用温度可达930 °C^[8-10],因为NiCr-Cr₃C₂涂层优异的性能,使其具有充当汽轮机各部件保护涂层的潜力.目前关于NiCr-Cr₃C₂涂层的制备及性能已有了众多的研究,Bobzin等^[11]利用氧气助燃超音速火焰喷涂(HVOF)技术制备了NiCr-Cr₃C₂涂层,并通过冲

击试验对该涂层进行评估,发现涂层在不同载荷下破裂机制不同,并且涂层的破裂会对基体产生更严重的磨损. Daniel等^[12]制备并研究了25% NiCr-Cr₃C₂涂层和50% NiCr-Cr₃C₂涂层的动态冲击磨损性能,发现在200 N的冲击载荷下50% NiCr-Cr₃C₂涂层冲击坑体积更大,但其冲击寿命高于25% NiCr-Cr₃C₂涂层.有研究人员研究了不同工艺对NiCr-Cr₃C₂涂层制备效果的影响,Bolelli等^[13]通过空气助燃超音速火焰喷涂(HVAF)和HVOF对不同粒度分布的NiCr-Cr₃C₂粉末进行了喷涂处理,并对生成的涂层进行了综合表征.程国东等^[14]探究了燃气流量对使用HVOF制备NiCr-Cr₃C₂涂层制备的影响.也有研究人员通过在NiCr-Cr₃C₂涂层中添加其他物质以提高涂层的性能,曹玉霞等^[15]在NiCr-Cr₃C₂涂层中添加了hBN(无机硼化物)作为固体润滑剂,发现NiCr/Cr₃C₂-hBN复合涂层呈层状结构,各层间结合良好,且涂层有着良好的抗热震性能.虽然已有众多对NiCr-Cr₃C₂涂层的研究,但关于该涂层在高温环境下的冲击磨损行为却鲜有研究.本文中汽轮机气缸配套件材料G115为基体,采用HVOF制备了2种不同

NiCr含量的NiCr-Cr₃C₂涂层, 在自研的高温铁屑冲击磨损试验机上研究了2种涂层在铁屑冲蚀环境下的高温冲击磨损行为, 通过改变冲击次数来探究2种涂层在冲击磨损过程中的冲击动力学响应和冲击磨损机制, 并对2种涂层的耐高温冲击磨粒磨损性能进行分析。

1 试验部分

1.1 试验材料及制备

本研究中采用的材料喷涂基体为G115钢, 规格为20 mm×10 mm×10 mm, 由东方汽轮机有限公司提供, 采用HVOF对试样进行喷涂, 喷涂NiCr含量(质量分数)分别为35%和25%的NiCr-Cr₃C₂粉, 粉末粒度约为5~35 μm。具体的喷涂工艺参数为空气压力0.586 MPa, 载气速率15 L/min, 送粉速率80 g/min, 喷涂速度600~800 mm/s, 喷涂层厚180~200 μm。G115钢基体的主要化学成分(质量分数)为82.25% Fe、0.15% C、3.9% Co、9.1% Cr、3.5% W和0.5% Si。制备后35% NiCr-Cr₃C₂涂层和25% NiCr-Cr₃C₂涂层的表截面形貌的扫描电子显微镜(SEM)照片及粗糙度值如图1所示, 2种涂层的表面粗糙度及厚度相差不大, 35% NiCr-Cr₃C₂涂层表面粗糙度和厚度分别为3.33 μm和258 μm, 25% NiCr-Cr₃C₂涂层表面粗糙度和厚度分别2.28 μm和264 μm, 试验前测得35% NiCr-Cr₃C₂和25% NiCr-Cr₃C₂涂层的硬度分别为878.7HV 和945.2HV。

图2所示为2种NiCr含量的NiCr-Cr₃C₂涂层X射线衍射(XRD)图谱, 2种涂层除了固有的NiCr和Cr₃C₂相以外, 还检测出了少量的Cr₇C₃相, 这可能是因为在利用喷射火焰加热Cr₃C₂或在涂层形成过程中, Cr₃C₂可能会发生相分解反应 $7Cr_3C_2 \rightarrow 3Cr_7C_3 + 5C$ ^[16-18]。此外, 衍射峰在40°、45°和52°附近存在宽化现象, 说明涂层中含有一定的非晶结构, 这主要由喷涂过程中高温粒子快速冷却所致^[18]。

1.2 试验设备及方法

试验装置如图3所示, 该装置是以自主研发的能量控制型冲击磨损试验机^[19-21]为基础, 通过添加高温马弗炉装置及铁屑装置来实现高温铁屑环境下的冲击磨损, 在冲击过程中, 采集系统的位移传感器与力传感器能分别采集到撞击前后冲头的速度及试样的受力。试验过程如下: (1)预先装好试样块、冲击球、高温马弗炉及漏斗装置; (2)接通马弗炉电源, 在达到预定温度后, 打开铁屑流量控制阀, 使铁屑以恒定速度流下, 由于新加入的铁屑会吸收部分热量, 需等炉内温度稳定后再启动音圈电机并进行试验; (3)音圈电机

启动后将进行往复直线运动, 电机通过带动弹簧拉杆使得动能块从原点向前移动; (4)当速度达预设速度(冲击速度)时, 电机将减速, 使得弹簧拉杆与动能块分离; (5)动能块继续向前运动并以恒定速度撞向试样后回弹; (6)撞击完成后, 音圈电机通过弹簧拉杆将动能块拉回初始位置, 完成1个周期的冲击动作。在冲击过程中的能量转换除了动能和形变外, 往往还存在摩擦热等其他形式的能量转换, 但普遍认为在低速撞击的条件下, 热能的一部分可忽略, 故本研究中假设冲击能量仅转换为动能和冲击过程中的能量损失(试样塑性变形和材料去除过程中消耗的能量), 由动能定理 $E=1/2 mv^2$ 计算动能块冲击前后的动能, 两者的差为冲击过程中的能量损失 ΔE ^[22-24]。

1.3 试验方案

试验选取球/平面接触形式, 冲击头采用直径为4.76 mm的氮化硅陶瓷球(显微硬度为2273HV), 试验试样为以G115钢为基体的35% NiCr-Cr₃C₂涂层以及25% NiCr-Cr₃C₂涂层, 试验动能块质量设定为700 g(含连接杆和撞头)。初始冲击速度设定为150 mm/s, 冲击次数 N 设定为 1×10^4 、 2×10^4 和 5×10^4 。磨粒为铁屑, 经人工破碎和筛选后得到粒径为380 μm的Fe₃O₄颗粒(在汽轮机服役过程中可能受金属氧化膜垢层的侵蚀), 试验温度为630 °C(汽轮机部件服役的环境温度)。

试验前, 用AFFRIDAKO 300维氏硬度计测量2种涂层在常温下的硬度。试验后, 使用Contour GT型白光干涉仪对磨痕的轮廓进行测量; 使用VHX-1000C型光学显微镜观察样品表面磨损情况; 使用JSM6610LV型扫描电子显微镜(SEM)观察磨痕表截面的微观形貌; 使用OXFRODX-Max80型能谱仪(EDS)分析仪观察磨痕表截面的元素分布。

2 结果与讨论

2.1 冲击动力学响应

每次冲击前的初始速度均为150 mm/s, 取不同冲击次数下最后1次冲击时的数值, 绘制35% NiCr-Cr₃C₂涂层和25% NiCr-Cr₃C₂涂层在不同冲击次数下的冲击动力学响应曲线, 如图4所示。不同冲击次数下2种涂层的冲击速度曲线如图4(a)和(b)所示, 可以看出冲击次数越大, 2种涂层的回弹速度越小, 即冲击前后速度变化值 $|\Delta v|$ 随冲击次数的增加而增大, 说明随着冲击次数的增加, 试样吸收的能量逐渐增大, 冲击前后动能变化量也越大^[25-26]。在相同冲击次数下, 25% NiCr-Cr₃C₂涂层的回弹速度大于35% NiCr-Cr₃C₂涂层的回弹速

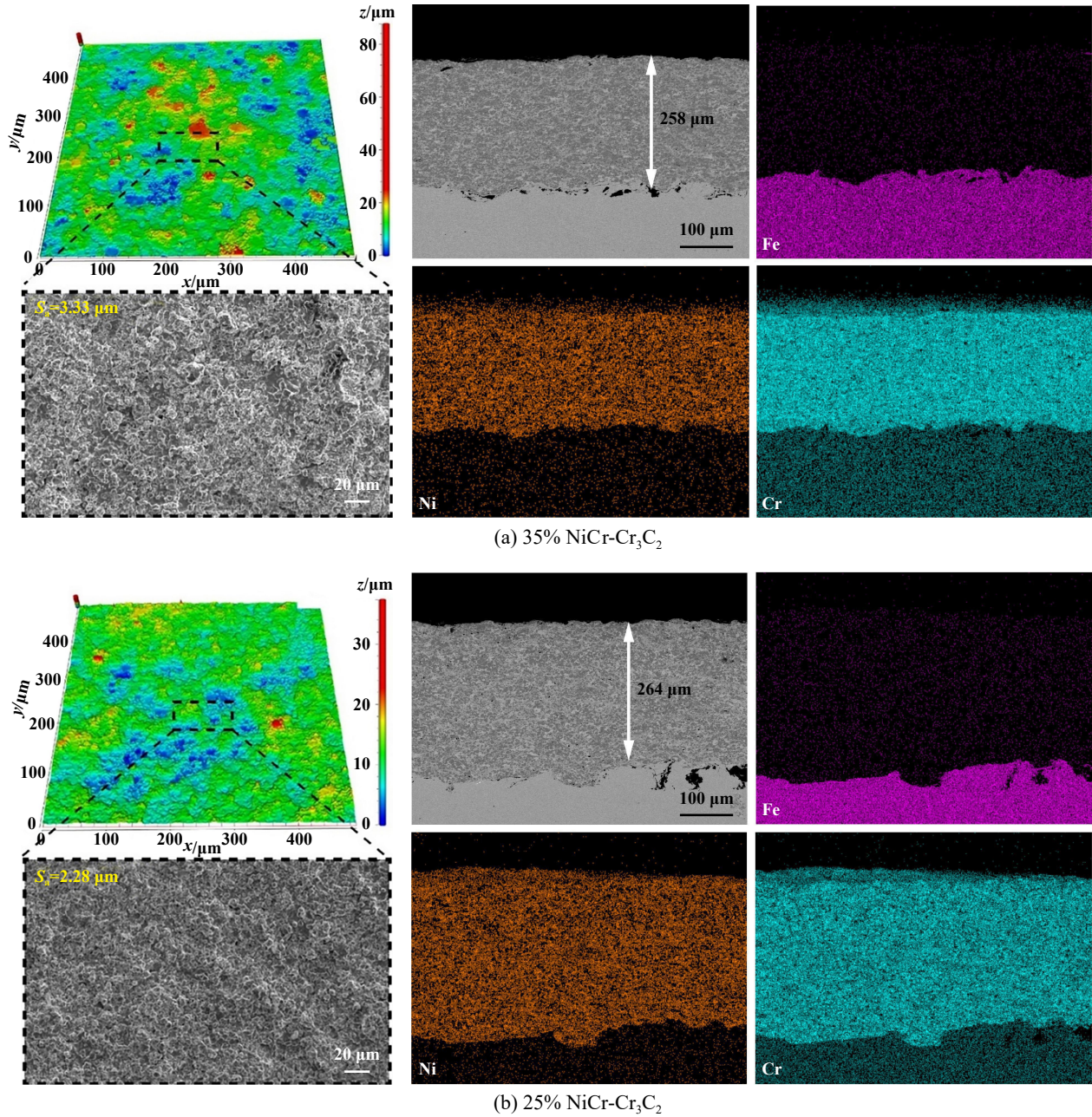


Fig. 1 3D morphology, SEM micrographs and element distributions of surface and cross-section morphology of two NiCr-Cr₃C₂ coatings

图1 2种NiCr-Cr₃C₂涂层表截面形貌的三维形貌图和SEM照片

度,说明25% NiCr-Cr₃C₂涂层在冲击过程中吸收的能量较少,该涂层发生了较轻的塑性变形和材料去除。这是因为材料的硬度越高,其耐磨损及抗变形能力越好,而25% NiCr-Cr₃C₂涂层碳含量较高,使其硬度较高,故表现出更好的抵抗塑性变形和材料去除的能力^[27]。图4(c)和(d)所示为2种涂层在不同冲击次数下的冲击力变化曲线,由于2种涂层材料性能有所差异,导致采集到的冲击力波形也有所不同^[28],但无论哪种涂层,其冲击力均随着冲击次数的增大而减小,这是因为在

持续冲击下材料的塑性变形量将增大,冲击球与试样的接触面积也随之增大,接触面积增大将减小试样所受接触应力,最终导致冲击力减小。在相同的冲击次数下,35% NiCr-Cr₃C₂涂层的冲击力明显较小,这是由于35% NiCr-Cr₃C₂涂层发生了更严重的塑性变形,使冲击球与试样的接触面积较大。

2种涂层的冲击能量曲线如图5(a)和(b)所示,可以看出在冲击过程中2种涂层的回弹速度随冲击次数的增大而减小,根据上文中所述回弹速度越小,能量损

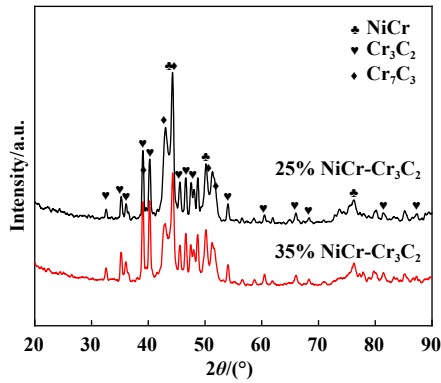


Fig. 2 XRD patterns of two NiCr-Cr₃C₂ coatings
图 2 2种NiCr-Cr₃C₂涂层XRD图谱

失 ΔE 越大,即2种涂层的能量损失 ΔE 随冲击次数增大而增大,这说明在冲击过程中,冲击耗散的能量随着冲击次数的增加而增加,有更多的能量被试样吸收用于塑性变形和材料去除^[29].图5(c)和(d)所示为不同冲击次数下2种涂层的能量吸收量和吸收率,2种涂层的能量吸收量和吸收率均随着冲击次数的增加而增大,并且在相同冲击次数下25% NiCr-Cr₃C₂涂层的吸收量和吸收率更小,说明该涂层抗高温铁屑冲击性能较好.

2.2 涂层冲击性能

图6所示为2种涂层在不同冲击次数下的磨痕形

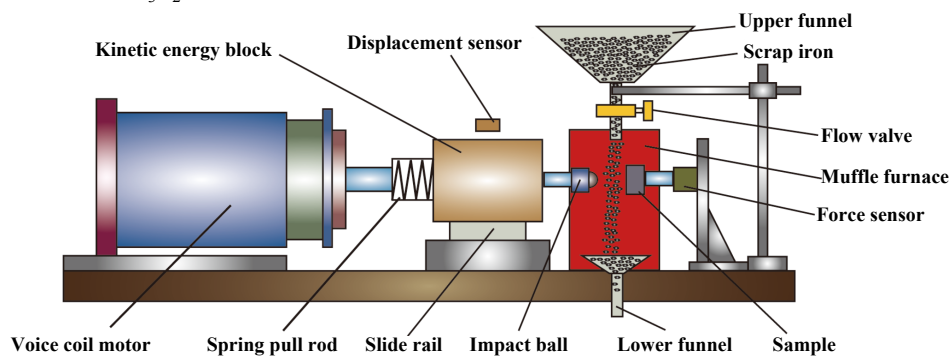


Fig. 3 Schematic diagram of high temperature iron chip impact wear testing machine
图 3 高温铁屑冲击磨损试验机示意图

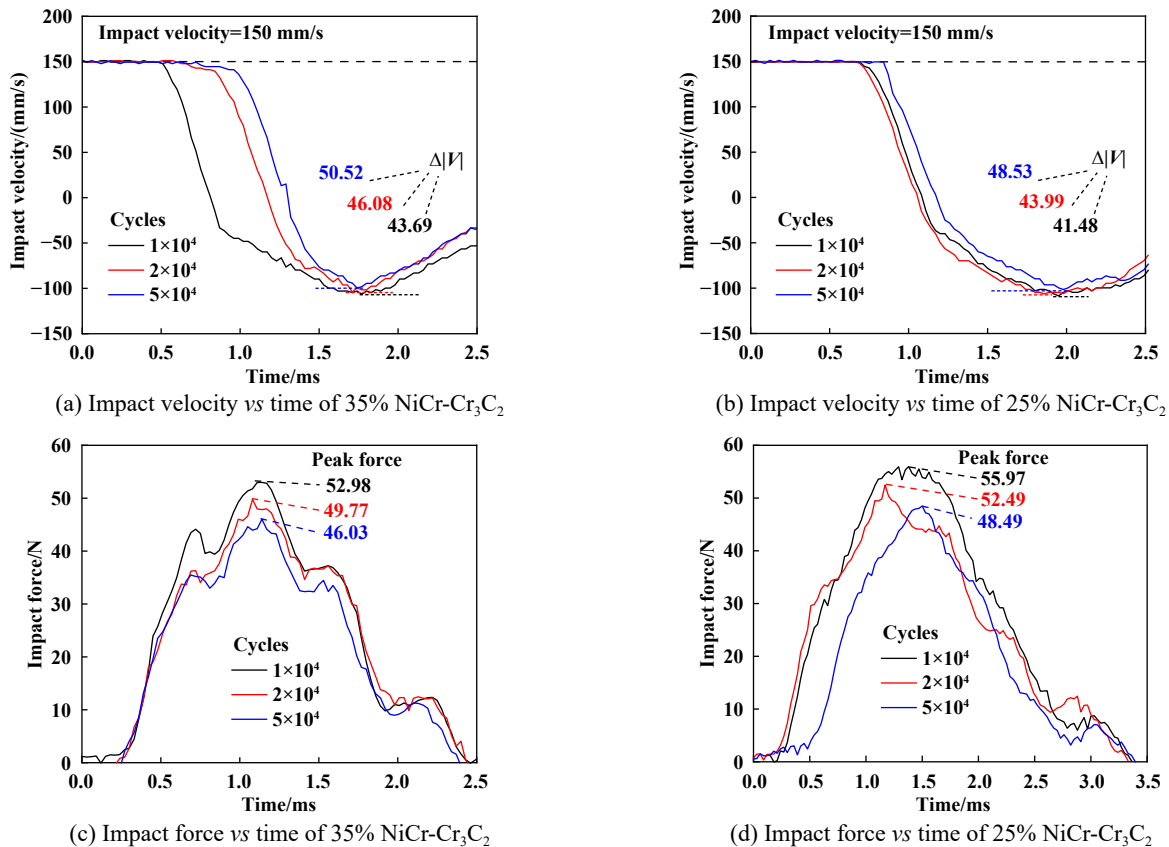


Fig. 4 Dynamic response curves of two NiCr-Cr₃C₂ coatings under different impact times

图 4 2种NiCr-Cr₃C₂涂层在不同冲击次数下的动力学响应曲线

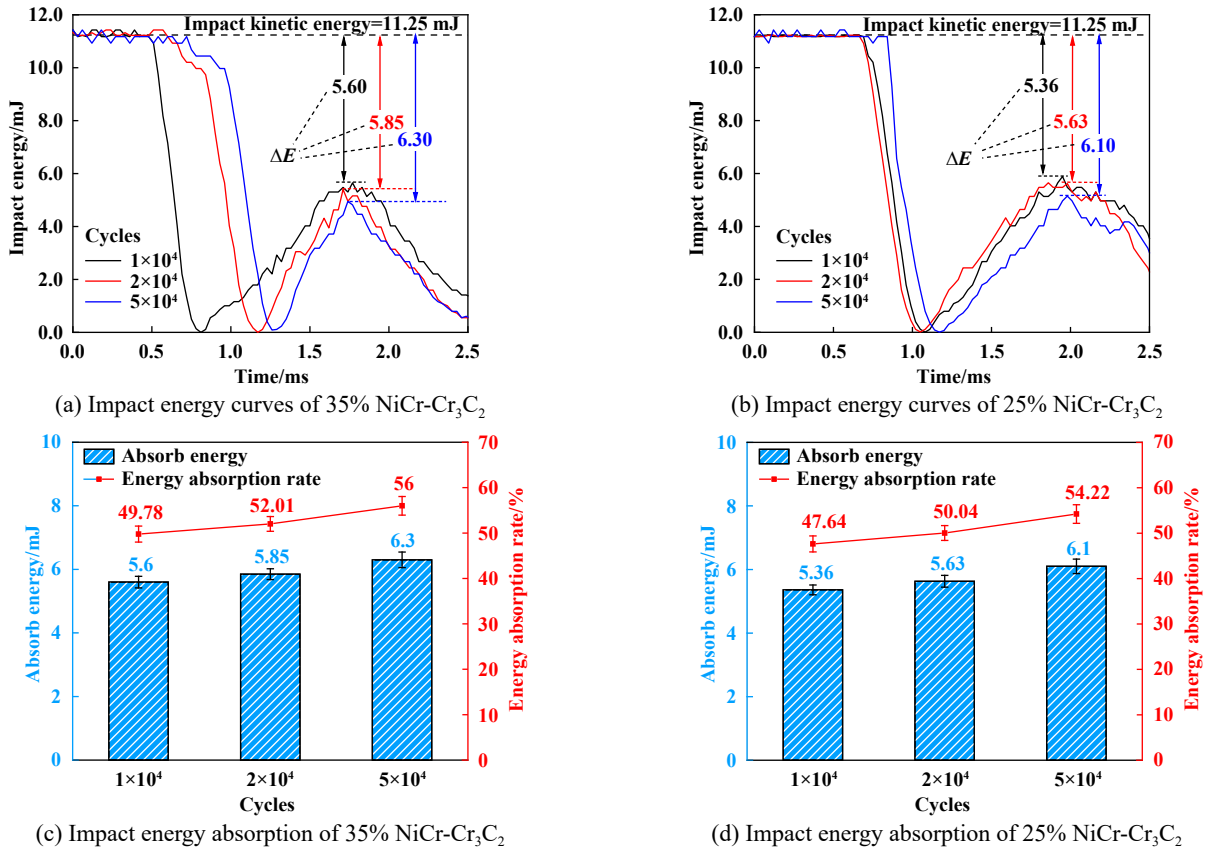


Fig. 5 Impact energy and absorb energy of two NiCr-Cr₃C₂ coatings at different impact times

图5 2种NiCr-Cr₃C₂涂层在不同冲击次数下的冲击能量和吸收能量曲线

貌的光学显微镜照片, 整个磨损区域可以分为由铁屑冲击形成的冲蚀磨损区域(红圈标注)以及由撞头直接接触形成的冲击磨损区域(蓝圈标注). 可以看出, 2种涂层的磨损区域均随着冲击次数的增加而增大, 当冲击次数从1×10⁴增长至5×10⁴时, 35% NiCr-Cr₃C₂涂层的冲蚀磨损区域直径(D)从3.241 mm增长至3.488 mm, 冲击磨损区域直径(d)从1.098 mm增长至1.310 mm, 两区域直径分别增长了7.62%和19.31%, 而25% NiCr-Cr₃C₂涂层的冲蚀磨损区域直径从3.348 mm增长至3.421 mm, 冲击磨损区域直径从1.104 mm增长至1.328 mm, 两区域分别增长了2.18%和20.29%.

图7(a)和(b)所示为2种涂层在不同冲击次数下的磨痕截面轮廓图, 可以看出, 35% NiCr-Cr₃C₂涂层的最大磨痕深度呈现先增大后减小的规律, 这是因为在冲击过程中产生的磨屑和作为磨粒的铁屑会堆积在磨痕周围及边缘, 并随着冲击次数的增加被逐渐压实, 成为在冲击球与试样间充当第三体的凸起物, 填充原本由塑性变形和材料去除后产生的凹坑, 进而出现最大磨痕深度随冲击次数增大而减小的现象. 25% NiCr-Cr₃C₂涂层的磨痕呈现出“W”型的轮廓, 说明在冲击过

程中发生了黏着磨损^[30], 这是因为25% NiCr-Cr₃C₂涂层硬度较高, 铁屑不易嵌入涂层表面, 而高温下铁屑具有良好的延展性, 更容易附着在涂层表面, 最终导致涂层产生黏着磨损.

图7(c)和(d)分别所示为2种涂层在不同冲击次数下的磨损面积和体积的统计值. 2种涂层的磨损面积如图7(c)所示, 2种涂层的磨损面积均随着冲击次数的增大而增大, 但在相同冲击次数下两者的磨损面积相差不大, 这是由于冲击球直径相同, 导致2种涂层在不同冲击次数下的磨损面积差异不大. 2种涂层磨损体积如图7(d)所示, 35% NiCr-Cr₃C₂涂层由于有堆积物的存在, 出现随着冲击次数的增大磨损体积先增大再减小的现象, 而25% NiCr-Cr₃C₂涂层磨损体积随冲击次数的增大而增大. 在相同的冲击次数下, 25% NiCr-Cr₃C₂涂层的磨损体积明显较小, 这是因为25% NiCr-Cr₃C₂涂层中碳化物含量较高, 从而具有较高的硬度以及较好耐磨性, 使得该涂层在冲击过程中更难以产生磨损.

图8所示为冲击次数为5×10⁴时2种涂层磨痕表面形貌的SEM照片和EDS结果, 磨痕表面不同位置的主要化学成分列于表1中. 根据EDS面扫数据发现2种涂

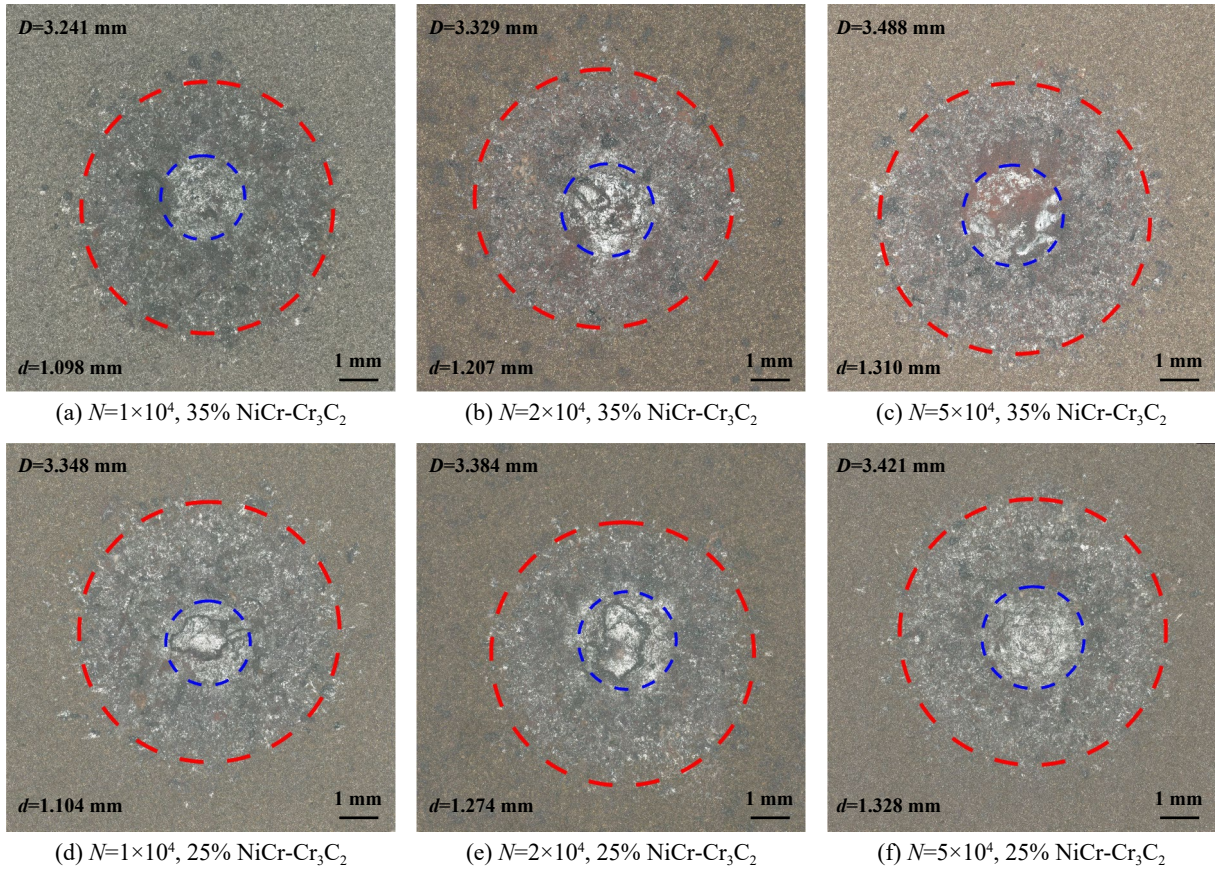


Fig. 6 Optical micrograph of wear morphologies of two NiCr-Cr₃C₂ coatings at different impact times

图 6 2种NiCr-Cr₃C₂涂层在不同冲击次数下的磨痕形貌的光学显微镜照片

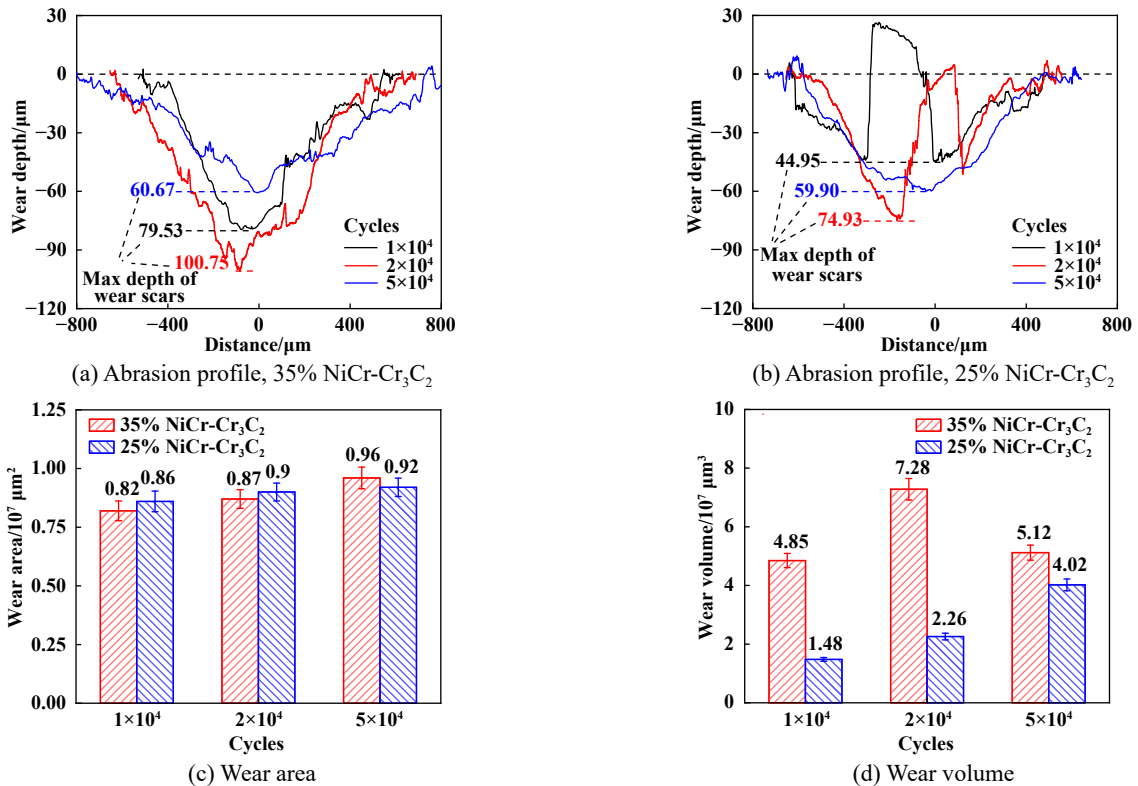


Fig. 7 Abrasion profile and wear data of two NiCr-Cr₃C₂ coatings under different impact cycles

图 7 2种NiCr-Cr₃C₂涂层在不同冲击次数下的磨痕截面轮廓和磨损数据

层表面有Fe元素富集现象, 这说明在冲击过程中有铁屑嵌入到了磨痕表面. 在2种涂层表面均检测到了Ni和Cr元素, 说明2种涂层在冲击过程中并未完全脱落, 具有抗高温铁屑冲击磨损的性能. 从SEM形貌照片观察到2种涂层磨痕区域并未发现铁屑切削磨痕表面的痕迹, 并且在35% NiCr-Cr₃C₂涂层的磨痕中心区域有众多凸起物存在, 在表1中A~D点均检测到大量Fe元素, 证实了铁屑填补了冲击产生的部分凹坑.

图9所示为在冲击次数为 5×10^4 下2种涂层磨痕截面形貌的SEM照片和EDS结果, 磨痕截面不同位置的主要化学成分列于表2中. 根据EDS图可发现2种涂层

在冲击过程中未完全剥落, 磨痕表面粘接着大量的铁屑, 也确实存在着堆积物, 根据SEM形貌照片可观察到堆积物的位置应处于冲击磨损区域的边缘和中心, 并且还可观察到由磨粒冲击形成的粗糙磨痕表面和剥落坑. 表2中的A和C点均检测到有Fe元素存在, 证明了磨痕表面有铁屑存在.

图10所示为2种涂层在高温铁屑环境下的损伤机理图, 2种涂层的主要损伤机理均为塑性变形以及磨粒磨损. 对于35% NiCr-Cr₃C₂涂层, 在冲击前期和中期, 冲击球的持续冲击使得涂层发生塑性变形, 同时作为磨粒的铁屑与试样表面相互接触产生摩擦磨损造

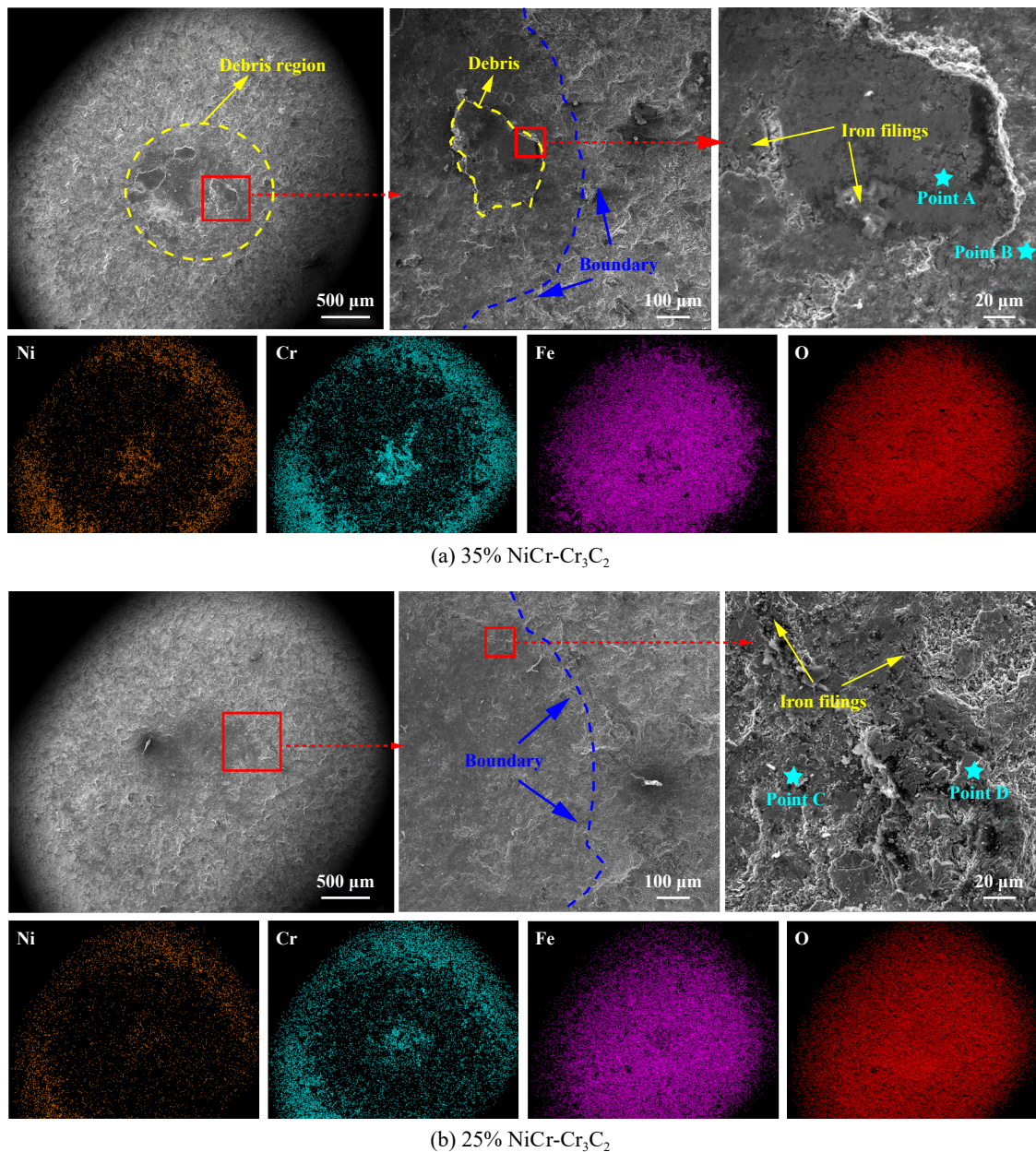


Fig. 8 SEM micrographs of morphology and EDS results of worn surface of two NiCr-Cr₃C₂ coatings ($N=5 \times 10^4$)

图8 2种NiCr-Cr₃C₂涂层磨痕表面形貌的SEM照片和EDS结果($N=5 \times 10^4$)

表 1 2种涂层磨痕表面不同位置的主要化学元素含量
Table 1 Main chemical components of two NiCr-Cr₃C₂ coatings at different positions on the surface of the wear marks

Point	Mass fraction/%				
	C	O	Fe	Ni	Cr
A	-	24.7	75.3	-	-
B	2.3	29.1	58.6	5.5	4.3
C	-	41.0	59.0	-	-
D	-	34.6	65.4	-	-

成了表面材料的磨粒磨损;当冲击达一定次数时进入到冲击后期,此时高温下具有良好延展性的金属铁屑同冲击产生的磨屑将在冲击力的作用下嵌入到磨痕表面并填补凹坑,在随后的冲击过程中被压实压紧形成堆

积物,堆积物成为冲击球与冲击试样之间的第三体.而25% NiCr-Cr₃C₂涂层由于硬度较高,使得铁屑在冲击前期和中期不易嵌入至涂层表面反而附着其上,所以导致涂层发生黏着磨损,产生“W”型轮廓的磨痕.在冲击后期,由于25% NiCr-Cr₃C₂涂层具有较好的耐磨性,其产生的磨损明显小于35% NiCr-Cr₃C₂涂层产生的磨损.

3 结论

系统地研究了2种NiCr含量的NiCr-Cr₃C₂涂层在高温铁屑环境下的冲击磨损行为,根据2种涂层冲击磨损过程中的冲击动力学响应及冲击后试样的磨痕形貌数据,分析了2种涂层的耐高温冲击磨粒磨损性

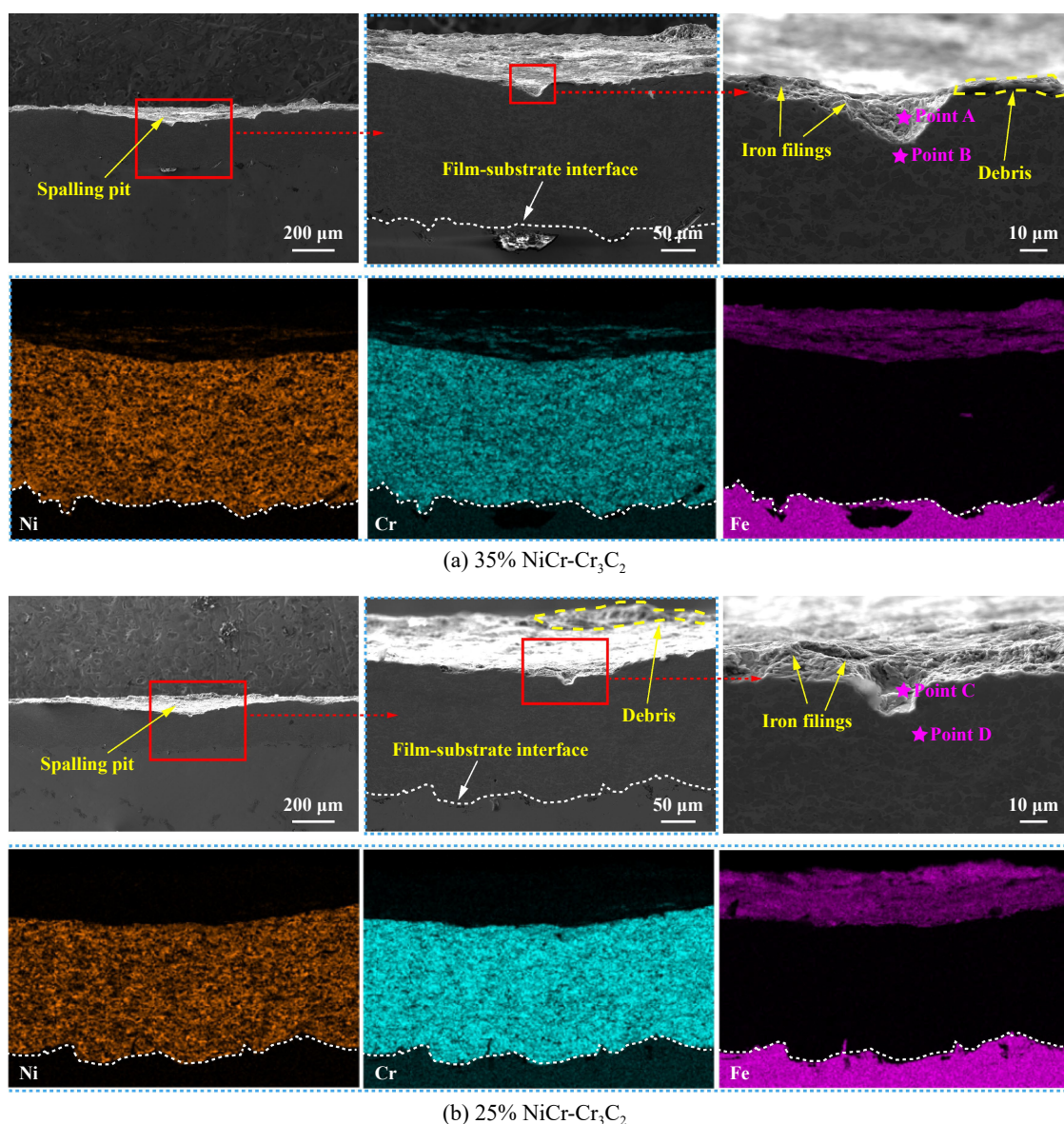


Fig. 9 SEM micrographs of morphology and EDS results of abrasion cross sections of two NiCr-Cr₃C₂ coatings ($N=5 \times 10^4$)

图9 2种NiCr-Cr₃C₂涂层磨痕截面的SEM形貌照片和EDS结果($N=5 \times 10^4$)

表2 磨痕截面不同位置的主要化学元素含量
Table 2 Main chemical components at different positions of the abrasion section

Point	Mass fraction/%				
	C	O	Fe	Ni	Cr
A	2.8	19.5	64.5	5.3	4.1
B	5.7	0.0	0.0	3.9	90.3
C	0.5	43.9	44.4	9.1	2.1
D	4.1	0.0	0.0	37.7	58.2

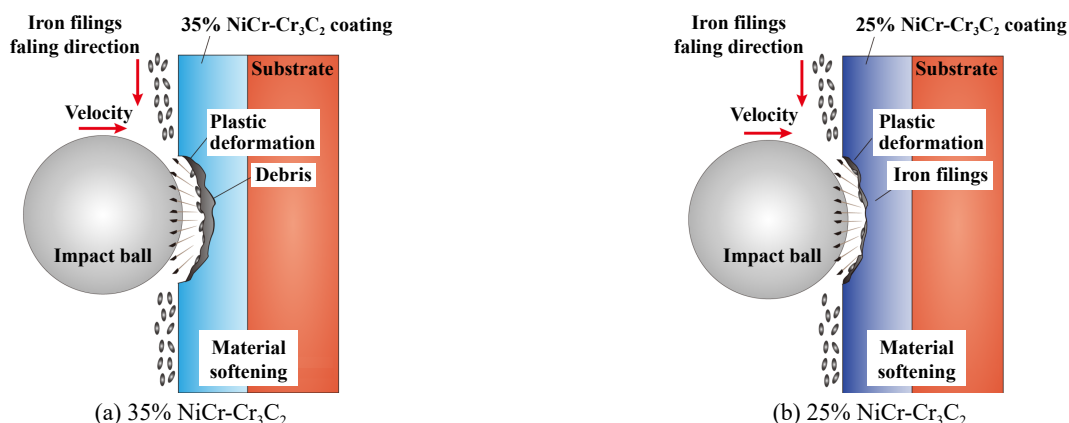


Fig. 10 Damage mechanism diagram of coating under wear

图10 涂层的冲击损伤机理图

能, 得到以下结论:

a. 在高温铁屑环境下, 35% NiCr-Cr₃C₂涂层和25% NiCr-Cr₃C₂涂层的损伤机理均为塑性变形和磨粒磨损, 并且在相同冲击次数下2种涂层的磨损面积相差不大. 随着冲击次数的增加, 2种涂层的冲击能量、能量吸收率及磨损面积均呈增长趋势, 冲击力的峰值呈下降趋势, 即随着冲击次数的增加, 2种涂层发生了更多的材料去除和塑性变形.

b. 25% NiCr-Cr₃C₂涂层的磨损体积随冲击次数的增加而增加, 并且在相同冲击次数下25% NiCr-Cr₃C₂涂层能量吸收量及吸收率和磨损体积均小于35% NiCr-Cr₃C₂涂层, 表现出更好的耐高温冲击磨粒磨损性能.

c. 在高温环境中铁屑具有良好的延展性易被冲击球压紧压实, 成为在冲击球与冲击试样间的第三体, 由于这种第三体的形成将填补磨痕上的部分凹坑, 导致35% NiCr-Cr₃C₂涂层的磨损体积随冲击次数的增加呈现先增大再减小的规律.

参考文献

[1] Shi Jinyuan, Li Jun, Liu Xia, et al. Research progress and prospect of large capacity steam turbine technology in China[J]. Journal of Chinese Society of Power Engineering, 2022, 42(6): 498-506 (in Chinese) [史进渊, 李军, 刘霞, 等. 我国大型汽轮机技术研究进展

与展望[J]. 动力工程学报, 2022, 42(6): 498-506]. doi: 10.19805/j.cnki.jcspe.2022.06.002.

- [2] Dolatabadi A M, Moslehi J, Pour M S, et al. Modified model of reduction condensing losses strategy into the wet steam flow considering efficient energy of steam turbine based on injection of nano-droplets[J]. Energy, 2022, 242: 122951. doi: 10.1016/j.energy.2021.122951.
- [3] Hu Pengfei, Meng Qingqiang, Fan Tiantian, et al. Dynamic response of turbine blade considering a droplet-wall interaction in wet steam region[J]. Energy, 2023, 265: 126323. doi: 10.1016/j.energy.2022.126323.
- [4] Fathyunes L, Mohtadi-Bonab M A. A review on the corrosion and fatigue failure of gas turbines[J]. Metals, 2023, 13(4): 701. doi: 10.3390/met13040701.
- [5] Rivaz A, Anijdan S H M, Moazami-Goudarzi M, et al. Damage causes and failure analysis of a steam turbine blade made of martensitic stainless steel after 72, 000 h of working[J]. Engineering Failure Analysis, 2022, 131: 105801. doi: 10.1016/j.engfailanal.2021.105801.
- [6] Li Changjiu. Applications, research progresses and future challenges of thermal spray technology[J]. Thermal Spray Technology, 2018, 10(4): 1-22 (in Chinese) [李长久. 热喷涂技术应用及研究进展与挑战[J]. 热喷涂技术, 2018, 10(4): 1-22]. doi: 10.3969/j.issn.1674-7127.2018.04.001.
- [7] Xu Yiren, Zhu Tianyi, Li Yongjian, et al. Wear behavior of cobalt-

- based alloy brush wire and chromium carbide coating at high linear speed[J]. *Tribology*, 2022, 42(6): 1216–1225 (in Chinese) [徐乙人, 祝天一, 李永健, 等. 钴基合金钢丝与碳化铬涂层高线速度磨损行为研究[J]. *摩擦学学报*, 2022, 42(6): 1216–1225]. doi: [10.16078/j.tribology.2021182](https://doi.org/10.16078/j.tribology.2021182).
- [8] Dzhurinskiy D, Babu A, Pathak P, et al. Microstructure and wear properties of atmospheric plasma-sprayed Cr₃C₂-NiCr composite coatings[J]. *Surface and Coatings Technology*, 2021, 428: 127904. doi: [10.1016/j.surfcoat.2021.127904](https://doi.org/10.1016/j.surfcoat.2021.127904).
- [9] Lu Haiyang, Shang Jiantong, Jia Xiujie, et al. Erosion and corrosion behavior of shrouded plasma sprayed Cr₃C₂-NiCr coating[J]. *Surface and Coatings Technology*, 2020, 388: 125534. doi: [10.1016/j.surfcoat.2020.125534](https://doi.org/10.1016/j.surfcoat.2020.125534).
- [10] Shang Lunlin, He Dongqing, Li Wensheng, et al. Preparation and tribological behavior of Cr₃C₂-NiCr/DLC duplex coating with high load-bearing and wear resistance[J]. *Tribology*, 2022, 42(4): 751–763 (in Chinese) [尚伦霖, 何东青, 李文生, 等. 高承载高耐磨 Cr₃C₂-NiCr/DLC 复合涂层制备及摩擦学行为[J]. *摩擦学学报*, 2022, 42(4): 751–763]. doi: [10.16078/j.tribology.2021274](https://doi.org/10.16078/j.tribology.2021274).
- [11] Bobzin K, Zhao L, Öte M, et al. Impact wear of an HVOF-sprayed Cr₃C₂-NiCr coating[J]. *International Journal of Refractory Metals and Hard Materials*, 2018, 70: 191–196. doi: [10.1016/j.ijrmhm.2017.10.011](https://doi.org/10.1016/j.ijrmhm.2017.10.011).
- [12] Daniel J, Grossman J, Houdková Š, et al. Impact wear of the protective Cr₃C₂-based HVOF-sprayed coatings[J]. *Materials*, 2020, 13(9): 2132. doi: [10.3390/ma13092132](https://doi.org/10.3390/ma13092132).
- [13] Bolelli G, Berger L M, Börner T, et al. Sliding and abrasive wear behaviour of HVOF- and HVAF-sprayed Cr₃C₂-NiCr hardmetal coatings[J]. *Wear*, 2016, 358–359: 32–50. doi: [10.1016/j.wear.2016.03.034](https://doi.org/10.1016/j.wear.2016.03.034).
- [14] Cheng Guodong, Wang Yinzen, Qin Qingbin. Effect of fuel flow on microstructure and erosion performance of HVOF sprayed Cr₃C₂-NiCr coating[J]. *China Surface Engineering*, 2008, 21(1): 41–44 (in Chinese) [程国东, 王引真, 秦清彬. 燃气流量对超音速火焰喷涂 Cr₃C₂-NiCr 涂层组织与冲蚀性能的影响[J]. *中国表面工程*, 2008, 21(1): 41–44]. doi: [10.3321/j.issn:1007-9289.2008.01.009](https://doi.org/10.3321/j.issn:1007-9289.2008.01.009).
- [15] Cao Yuxia, Huang Chuanbing, Du Lingzhong, et al. Effects of hBN content on thermal shock resistance and oxidation properties of NiCr/Cr₃C₂-hBN composite coatings[J]. *China Surface Engineering*, 2015, 28(3): 17–22 (in Chinese) [曹玉霞, 黄传兵, 杜令忠, 等. hBN 含量对 NiCr/Cr₃C₂-hBN 复合涂层抗热震性能和氧化性能的影响[J]. *中国表面工程*, 2015, 28(3): 17–22]. doi: [10.11933/j.issn.1007-9289.2015.03.003](https://doi.org/10.11933/j.issn.1007-9289.2015.03.003).
- [16] Shi Chenxi, Liu Shibin, Irfan, et al. Deposition mechanisms and characteristics of nano-modified multimodal Cr₃C₂-NiCr coatings sprayed by HVOF[J]. *Reviews on Advanced Materials Science*, 2022, 61(1): 526–538. doi: [10.1515/rams-2022-0042](https://doi.org/10.1515/rams-2022-0042).
- [17] Meng Lingyu, Zhao Hanqing, Hu Ming, et al. Effect of laser remelting on microstructure and properties of Cr₃C₂-NiCr coating sprayed by supersonic flame[J]. *Hot Working Technology*, 2022, 51(20): 39–42 (in Chinese) [孟玲玉, 赵汉卿, 胡明, 等. 激光重熔对超音速火焰喷涂 Cr₃C₂-NiCr 涂层组织和性能的影响[J]. *热加工工艺*, 2022, 51(20): 39–42]. doi: [10.14158/j.cnki.1001-3814.20212699](https://doi.org/10.14158/j.cnki.1001-3814.20212699).
- [18] Shi Mengchuan, Xue Zhaolu, Liang Heping, et al. High velocity oxygen fuel sprayed Cr₃C₂-NiCr coatings against Na₂SO₄ hot corrosion at different temperatures[J]. *Ceramics International*, 2020, 46(15): 23629–23635. doi: [10.1016/j.ceramint.2020.06.135](https://doi.org/10.1016/j.ceramint.2020.06.135).
- [19] Lin Yingwu, Cai Zhenbing, Chen Zhiqiang, et al. Influence of diameter-thickness ratio on alloy Zr-4 tube under low-energy impact fretting wear[J]. *Materials Today Communications*, 2016, 8: 79–90. doi: [10.1016/j.mtcomm.2016.06.003](https://doi.org/10.1016/j.mtcomm.2016.06.003).
- [20] Chen Xudong, Wang Liwen, Yang Lingyun, et al. Investigation on the impact wear behavior of 2.25Cr-1Mo steel at elevated temperature[J]. *Wear*, 2021, 476: 203740. doi: [10.1016/j.wear.2021.203740](https://doi.org/10.1016/j.wear.2021.203740).
- [21] Wang Zhang, Cai Zhenbing, Chen Zhiqiang, et al. Correction to: low-velocity impact wear behavior of ball-to-flat contact under constant kinetic energy[J]. *Journal of Materials Engineering and Performance*, 2017, 26(11): 5680. doi: [10.1007/s11665-017-3002-2](https://doi.org/10.1007/s11665-017-3002-2).
- [22] Wang Haoyu, Cao Xiaoying, Li Dingjun, et al. Impact abrasive wear of CoCrWSi coating at high temperature[J]. *China Surface Engineering*, 2023, 36(3): 193–204 (in Chinese) [王浩宇, 曹晓英, 李定骏, 等. CoCrWSi 涂层高温冲击磨粒磨损行为[J]. *中国表面工程*, 2023, 36(3): 193–204]. doi: [10.11933/j.issn.1007-9289.20221017001](https://doi.org/10.11933/j.issn.1007-9289.20221017001).
- [23] Ji Dehui, Zhuang Hui, Hu Qiang, et al. Effect of abrasive particle size on the tribological behavior of thermal sprayed WC-Cr₃C₂-Ni coatings[J]. *Journal of Alloys and Compounds*, 2022, 924: 166536. doi: [10.1016/j.jallcom.2022.166536](https://doi.org/10.1016/j.jallcom.2022.166536).
- [24] Liu Shaopeng, Mei Lang, Shen Mingxue, et al. Effect of initial kinetic energy of Si₃N₄ ball on impact wear behavior of high-velocity oxygen fuel-sprayed WC-10Co-4Cr coating and medium-carbon steel[J]. *Journal of Materials Engineering and Performance*, 2023, 32(16): 7285–7296. doi: [10.1007/s11665-022-07633-3](https://doi.org/10.1007/s11665-022-07633-3).
- [25] Wang Zhang, Cai Zhenbing, Sun Yang, et al. Dynamic response and wear behavior of Cr-DLC coating under impact kinetic energy controlled mode[J]. *China Surface Engineering*, 2017, 30(4): 78–86 (in Chinese) [王璋, 蔡振兵, 孙阳, 等. 基于冲击动能控制的 Cr-DLC 涂层动力学响应和磨损行为[J]. *中国表面工程*, 2017, 30(4): 78–86]. doi: [10.11933/j.issn.1007-9289.20170220004](https://doi.org/10.11933/j.issn.1007-9289.20170220004).
- [26] Yu Tianda, Fu Guozhong, Yu Yanqing, et al. Wear characteristics of the nuclear control rod drive mechanism (CRDM) movable latch serviced in high temperature water[J]. *Chinese Journal of*

- Mechanical Engineering, 2022, 35(1): 26. doi: [10.1186/s10033-022-00695-3](https://doi.org/10.1186/s10033-022-00695-3).
- [27] Wang Shuoyu, Chen Pengfei, Cai Fei, et al. The study of HVOF Sprayed NiCr-Cr₃C₂ coatings with different carbide contents[J]. Thermal Spraying Technology, 2019, 9(2): 22–27,47 (in Chinese) [王硕煜, 陈鹏飞, 蔡飞, 等. HVOF喷涂不同碳化物含量的NiCr-Cr₃C₂涂层研究[J]. 热喷涂技术, 2019, 9(2): 22–27,47].
- [28] Wu Songbo, Cai Zhenbing, Lin Yu, et al. Effect of hard sand on the impact wear behavior of TC4 alloy[J]. Tribology, 2018, 38(4): 383–390 (in Chinese) [吴松波, 蔡振兵, 林禹, 等. 硬质沙粒对TC4钛合金冲击磨损的损伤行为的研究[J]. 摩擦学学报, 2018, 38(4): 383–390]. doi: [10.16078/j.tribology.2018.04.002](https://doi.org/10.16078/j.tribology.2018.04.002).
- [29] Xiang Pengcheng, Jiang Wenjuan, Ding Haohao, et al. Investigation on impact wear and damage properties of rail welded joints after two types of heat-treatments[J]. Tribology, 2021, 41(3): 382–392 (in Chinese) [向鹏程, 蒋文娟, 丁昊昊, 等. 2种热处理钢轨焊接接头冲击磨损与损伤性能研究[J]. 摩擦学学报, 2021, 41(3): 382–392]. doi: [10.16078/j.tribology.2020142](https://doi.org/10.16078/j.tribology.2020142).
- [30] Yu Yanqing, Chen Xudong, Yang Lingyun, et al. Investigation on fretting wear behavior of 2.25Cr-1Mo tube in water at various temperatures[J]. Wear, 2021, 476: 203727. doi: [10.1016/j.wear.2021.203727](https://doi.org/10.1016/j.wear.2021.203727).